GNSS Shadow Matching based on Intelligent LOS/NLOS Classifier

Conference Paper · December 2018

CITATIONS
7

READS
780

4 authors:

Haosheng Xu
The Hong Kong Polytechnic University
8 PUBLICATIONS **74** CITATIONS
SEE PROFILE

Guohao Zhang
The Hong Kong Polytechnic University
45 PUBLICATIONS **761** CITATIONS
SEE PROFILE

Bing Xu
The Hong Kong Polytechnic University
40 PUBLICATIONS **282** CITATIONS
SEE PROFILE

Li-Ta Hsu
The Hong Kong Polytechnic University
205 PUBLICATIONS **3,275** CITATIONS
SEE PROFILE

GNSS Shadow Matching based on Intelligent LOS/NLOS Classifier

Haosheng XU
Department of Mechanical Engineering
The Hong Kong Polytechnic University
Hong Kong
17074845g@connect.polyu.hk, guo-hao.zhang@connect.polyu.hk

Guohao ZHANG, Bing XU, Li-Ta HSU
Interdisciplinary Division of Aeronautical and Aviation Engineering
The Hong Kong Polytechnic University
Hong Kong
guo-hao.zhang@connect.polyu.hk; pbing.xu@polyu.edu.hk
lt.hsu@polyu.edu.hk

***Abstract*—It's well known that Global Navigation Satellite System (GNSS) is inaccurate in urban areas, because of many building blocked and/or reflected satellite signals. GNSS shadow matching is a promising positioning technique to improve the GNSS positioning accuracy in urbanized cities. Shadow matching algorithm is initialized by the positioning solution of conventional weighted least square estimation. Then, a grid map is defined. Shadow matching algorithm generates a building boundaries with the help of 3D city model to predict the satellite visibility (whether the direct signal transmission is visible or blocked) of the hypothesis locations in the grid map. By comparing the predicted with observed satellite visibilities at each gird point, a score for each grid point in the search area would be computed. The final positioning solution is calculated based the weighted average of the hypothesis locations, where the weighting is set based by the match score. However, it remains great challenges to identify whether the received GNSS measurements are through line-of-sight (LOS) or none-line-of-sight (NLOS) transmission in urban canyons because the NLOS signals could be received by reflection from buildings. LOS/NLOS classifier trained by machine learning algorithms would give higher recognition rate than the classifier solely based on received signal strength. This paper demonstrates the integration of GNSS shadow matching with the proposed intelligent LOS/NLOS classifier. The LOS/NLOS classifier based on signal to noise ratio (SNR), number of received satellites (NRS), elevation angle (EA), pseudorange residual (PR), pseudorange residual percentage (PRP) and normalized pseudorange residual (NRP). Different machine learning algorithms including k-nearest neighbors (KNN), neural network (NN), support vector machine (SVM), decision tree (TREE) and simple SNR classifier (SSC) algorithms will be implemented and compared. Different scenarios are also considered and used as training data, including mild or middle and deep urban areas with various building distributions. The classification accuracy of SSC considering C/N0 larger than 35 dB-Hz as LOS and smaller than 35 dB-Hz as NLOS, is 69.50% at deep urban areas, and 86.47% at middle or mild urban areas. Using data collected by a u-blox GNSS receiver in dense building areas of Hong Kong, the integrated shadow matching position solutions with the machine learning classifier are more accurate than weighted least squares (WLS)approach. The mean position error using intelligent LOS/NLOS classifier is reduced to 60% of that obtained using WLS.**

Keywords—GNSS, Smartphone, Shadow Matching, NLOS and Machine Learning

I. INTRODUCTION

Global Navigation Satellites Systems (GNSS) are widely applied in various scenarios and positioning services, e.g. vehicle or pedestrian navigation, which are frequently used in urban canyons. It is well-known, however, GNSS receivers show degraded performance under poor satellite geometric distribution due to the surrounding high-rise buildings in these areas [1].

Many technologies have been used to solve this problem, such as ray-tracking [2], pseudo-range error modelling [3], shadow matching (SM) [4], consistency checking [5], etc. Among these, the shadow matching method significantly outperforms conventional methods in cross-street direction determination [6]. With the help of 3D-mapping, shadow matching shows the potentials to give a four-time improvement on conventional GNSS solutions for both u-blox and smartphone receivers [7]. In recent year, machine learning technology has been used in GNSS fields.

The SDM method determines a user's position by comparing the similarities of satellite visibility between the receiver and the candidate positions. Both light-of-sight (LOS) and non-light-of-sight (NLOS) satellites contribute to the position determination. Thus, LOS/NLOS classifying performance has a great impact on the positioning accuracy.

In[8], machine learning technology was applied for estimating GPS observation errors in forestry environments and evaluating the effects of forest cover on positioning accuracy. Guinness [9] investigated a wide range of learning techniques for sensing mobility contexts, together with other sensors, e.g. GPS and accelerometers. The other integrations with GNSS are identifying mobility contexts. In [10], machine learning is used to detect ionospheric scintillation and classify scintillation events in the frequency domain. In this paper, the machine learning method is used to classify LOS/NLOS signals for SDM. In [6], signal-to noise-ratio (SNR) was used as the probability of LOS with Bayes theorem and fitting approach. Unfortunately, in urban canyons, a classifier based only on the SNR cannot determine satellite visibilities correctly. Thus, to distinguish between LOS and NLOS, multiple derivations from GNSS measurements should be jointly used. In this paper, the machine learning is trained using the following derivations: signal to noise ratio (SNR), number of received satellites (NRS), elevation angle (EA), pseudorange residual (PR), pseudorange residual percentage (PRP) and normalized pseudorange residual (NRP). The training models include k-nearest neighbors (KNN), neural network (NN), support vector machine (SVM), decision tree (TREE) and simple SNR classifier (SSC), corresponding to different building block shapes.

The rest of the paper is organized as follows: The model of NLOS/LOS classifier based on machine learning with different

feature selections and combinations would be introduced in Section II. After that shadow matching based machine learning technology would be expounded in Section III. The detailed experiments set-up and results are given in Section IV. Section V summarizes the conclusions and future work.

II. LOS/NLOS CLASSIFIER BASED ON MATCHING LEARNING

A. *Intelligent LOS/NLOS classifier based on machine learning*

The flowchart of the proposed classifier based on machine learning is shown in Fig. 1. In the offline stage, raw GNSS measurements are first collected in several urban scenarios, from which features are extracted. Then, satellite visibility are determined using the information of 3D building models, ground truth and GNSS ephemeris. Finally, an offline labelled database is generated, which contains a large amount of NLOS signals, because there are many surfaces reflecting or blocking the satellite signals. In the online stage, based on the offline database, an intelligent LOS/NLOS classifier based on machine learning is exploited. To accomplish this, features are extracted from the unlabeled GNSS measurements in real time, and used by machine learning classifier to detect LOS/NLOS signals.

B. *Features of model*

The GNSS measurements are provided in the form of Receiver Independent Exchange Format (RINEX) data, which consists of measuring time, pseudorange, carrier-phase and Doppler shift, etc. In this paper, all used machine learning features could be derived from raw RINEX data, which means that this approach can deal with a large number of measurements. Furthermore, there are some features presenting potential ability to discriminate NLOS and LOS signals as follows:

1) *Signal Noise Ratio (SNR)*

It has been proved that LOS signals have higher SNR than NLOS signals in most cases [6]. Therefore, SNR is usually used as a feature for LOS signals. In our training dataset, similar phenomenon has also been observed as shown in Fig. 2.

2) *Number of received satellites (NRS)*

The number of received satellites is obtained directly from RINEX file.

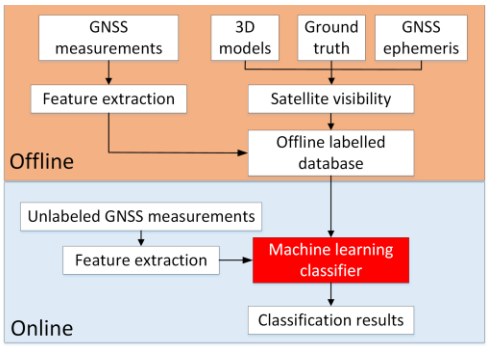

Fig. 1. Flowchart of intelligent LOS/NLOS classifier based on machine learning.

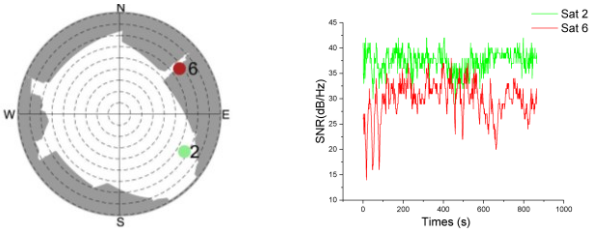

(a) Skymask of LOS/NLOS satellites (b) SNR value of LOS/NLOS signals

Fig. 2. Demonstration of SNR of LOS/NLOS signals.

3) *Elevation angle (EA)*

NLOS effect is highly correlated with the satellite elevation angle [11]. Thus, the EA is used as a feature for training the machine learning model.

4) *Pseudorange Residual (PR)*

The position estimation is obtained using the least square method as following:

$$X = \left(H^T H\right)^{-1} H^T p \tag{1}$$

where X is receiver state, H is a matrix composed of unit vectors pointing from the user to satellites in ECEF coordination and clock bias. p denotes pseudorange measurements. After several iterations, a more accurate position could be generated and the pseudorange residual is calculated by :

$$PR = p - H \cdot X \tag{2}$$

5) *Pseudorange Residual Percentage (PRP)*

A pseudorange residual percentage, PRP (%), is defined as the constitute percentage of mean value of pseudorange residual at each epoch:

$$PRP = \frac{Pr_i \cdot n}{\sum_i^n \cdot Pr_i} \tag{3}$$

where n is the received satellite number.

6) *Normalized Pseudorange Residual (NPR)*

Moreover, at each epoch, the pseudorange residual for satellite i can be normalized by:

$$NPR = \frac{Pr_i - Pr_{\min}}{Pr_{\max} - Pr_{\min}} \tag{4}$$

$Pr_{\max}$ and $Pr_{\min}$ are the maximum and minimum pseudorange residuals for all satellites at each epoch.

III. SHADOW MATCHING BASED ON MACHINE LEARNING

The flowchart of shadow matching algorithm based on machine learning is shown in Fig. 3. The module in red is the newly proposed method in this paper, compared with the basic shadow matching algorithm [4]. Main modules are described as follows:

1) *Search area determination*

An 50 square meters search area is created, centering at the initial weighted least square position solution with GNSS measurement. Within this search area, the building

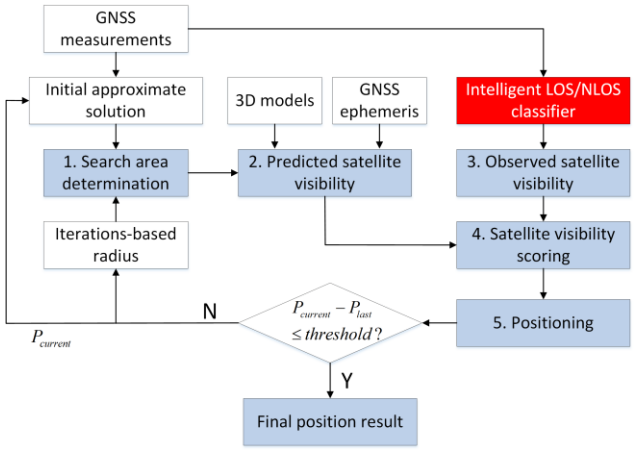

Fig. 3. Flowchart of shadow matching algorithm with machine learning.

boundary information and a gird map with a 2-meter resolution are also generated.

2) *Predicted satellite visibility*

As shown in Fig. 4, in dense urban areas, signals from satellites with low elevation angles are likely to be blocked by surrounding tall buildings, leading to the satellite invisibility. Thus, a straightforward and effective way to predict satellite visibility is comparing the elevation angles of both satellites and building boundaries at the same azimuth angle. 3D building models and GNSS measurements are used to obtain the building boundary information and satellites position, respectively.

3) *Observed satellite visibility*

For observed satellite visibility, one of the convenient ways is to consider all received signals as LOS (tracked) signals, but actually the measurements may include both NLOS and LOS signals [12]. Another approach is using a SNR-weighted fitting model to predict the probability of LOS signals [6]. Signal strength can also be considered as a distinctive feature of NLOS/LOS. However, those attempts still face the difficulty in various scenarios with unreliable SNR value. In this paper, all the received signal would be classified using machine learning technology described in Section II, which is also is a contribution of this paper.

4) *Score scheme*

Basing on the observed and predicted satellite visibility, a score scheme for candidate locations is needed. At one candidate position, a satellite predicted to be unblocked by buildings, if and only if it is measured and classified as LOS signal would gain a point. On the other hand, for predicted blocked satellite, only by meet the requirement of NLOS labelled or not measured, the satellite would also gain a point for this candidate position as shown in Fig. 5.

5) *Positioning*

The final position solution is set to the weighted mean of the highest scoring candidate positions. At the same time, this solution would be considered as an initial position for next loop till there is a very small difference between the last and current solutions, and the radius of searching circle will be decreased to migrate the impact of local Minima. For this case, local Minima means similar building scenarios but far away position or satellite geometry makes shadow matching score becomes very close or even same, which could decrease shadow matching accuracy as shown in Fig. 6.

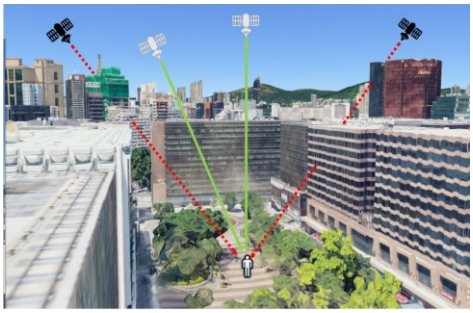

Fig. 4. Demonstration of signal blockage.

Fig. 5. Demonstration of score scheme.

IV. Experiments and Analysis

A. Experimental set-up

GNSS raw data was collected at seven different locations in an urban area of Kowloon in Hong Kong, as shown in Fig. 7. At each location, static data was collected for more than 10 minutes using a u-blox NEO M8T receiver.

The seven locations contain most types of building blocking circumstances. According to the number of building sides which surround the location, the seven locations are divided into four groups. Group 1 contains Location 1, which is blocked by one building side. Group 2 contains Locations 2 to 5, which are blocked by two sides. Location 6 represents a deep urban environment with 3 surrounding buildings in its front, belonging to Group 3. Location 7, divided into Group 4, is the deepest urban canyon among the seven locations, where only satellites with very high elevation angles are receivable. Skymasks of the above four groups are shown in Fig. 8.

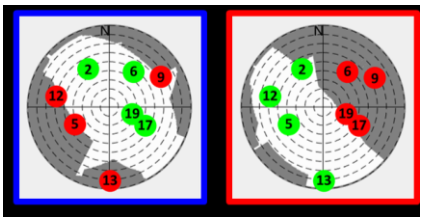

Fig. 6. Different locations with the same matching score.

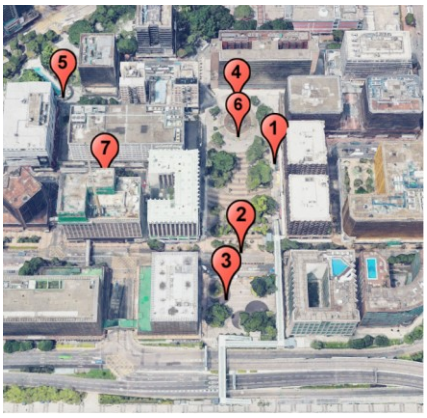

Fig. 7. Experiment area in Hong Kong.

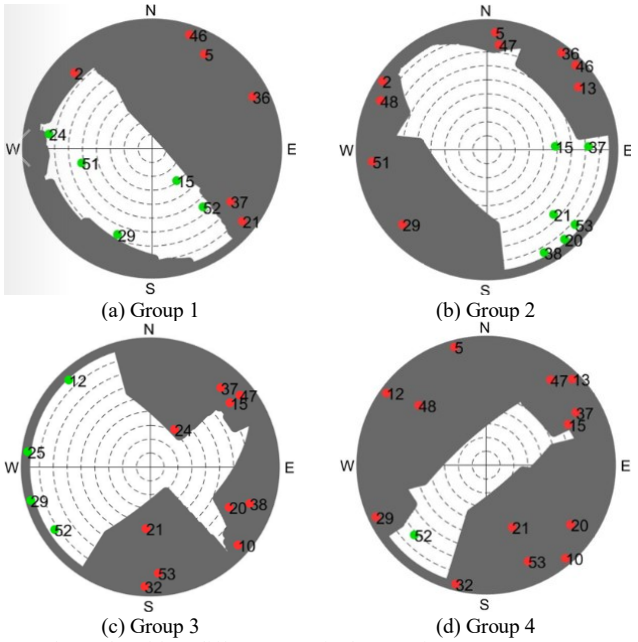

(a) Group 1 (b) Group 2

(c) Group 3 (d) Group 4

Fig. 8. Skymasks of four different cases in the experiments.

Table I lists the detailed information of data collected in different locations, L1 to L7. LA and LB are two locations to test the training model, as shown in Fig. 9. Location A is in the middle of an square, intended for testing the machine learning performance in areas where two or three building sides exist.

Compared to Location A, Location B is closer to one side of the area, which represents the cases of one or two building sides.

B. Results and analysis

1) Classification results

Features are also divided into several groups to explore which features contribute more to machine learning based classifier, as shown in Table II.

After obtaining the features from raw GNSS measurements at training locations, the machine learning models are modified and then tested at Location A and B, with results shown in Tables III and IV, respectively.

From Table III, it could be noted that SVM have the best performance over all the results as 78.31% percentage to predict the right type of signals. Furthermore, most models have similar performance only based SNR feature, approximately 70%. In addition, we have found that when taking elevation angle into model, performance of KNN, SVM and TREE have improved a lot, even 20% in TREE model and almost 10% in KNN. That bring us the idea that besides the SNR value, elevation angle could play an important role in classification. However, the pseudorange residual, pseudorange residual percentage ratio and pseudorange residual rate could not help to improve the model a lot, or even getting worse for KNN, SVM and NN. The more intuitive result is shown in Fig. 10.

At areas with fewer surrounding sides blocked, e.g. Location B, the classification accuracy improves a lot for most of feature

TABLE I. SUMMARY OF THE DATASETS

Number of blocked sides	*Dataset Number*	*Dataset type*	*Total samples*	*LOS (-1)*	*NLOS (1)*	*LOS rate (%)*
1	L1	Training	6066	3972	2094	65.48
2	L2	Training	11081	6059	5022	54.68
2	L3	Training	15805	7744	8061	49.00
2	L4	Training	8889	3102	5787	34.09
2	L5	Training	18027	5568	12459	30.89
3	L6	Training	13020	8428	4592	33.35
4	L7	Training	13440	2532	10908	18.84
2~3	LA	Testing	9900	5370	4530	54.24
1~2	LB	Testing	13900	7698	5833	55.38

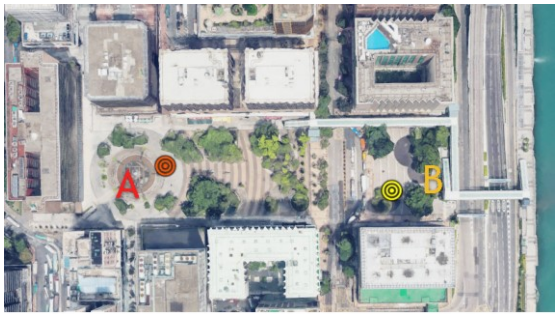

Fig. 9. Two locations to test.

groups and machine learning models, as shown in Table IV. For example, for feature group 1 (i.e. only SNR) and NN model, the maximum accuracy is approximately 90%. Furthermore, it can be found that the accuracy for Simple SNR Classifier (SSC) also has a very high percentage as 86.47%. Both phenomena indicate that SNR value could be a major factor affecting the machine learning result in middle and mild urban environment. When more features are used, however, the accuracy decreases greatly for most models, especially for KNN, NN and TREE. For SVM, the accuracy decreases slightly. Furthermore, the pseudorange residual may improve the accuracy, with almost 8% improvement for KNN and TREE and 19% improvement for NN, respectively. The more intuitive result bar is shown in Fig. 11.

2) Positioning results

After obtaining the LOS/NLOS classification results based on machine learning technology, positions are fixed using shadow matching method for Locations A and B, with results shown in Tables V and VI, respectively. The tables also list the classification accuracy results. SVM with feature group 3 and SVM with feature group 1 are used for Locations A and B, respectively. For comparison, the positioning results of weighted least square (WLS) and SM with 100% of classification accuracy (True label) are also shown.

TABLE II. FEATURE GROUPS

Feature group	*Features*					
	SNR	*NRS*	*EA*	*PR*	*PRP*	*NPR*
1	√					
2	√	√				
3	√	√	√			
4	√	√	√			
5	√	√	√	√	√	
6	√	√	√	√		√
7	√	√	√	√	√	√

TABLE III. CLASSIFICATION RESULTS AT LOCATION A

Feature group	*Classification accuracy at LA (%)*				
	KNN	*NN*	*SVM*	*TREE*	*SSC*
1	57.23	70.43	69.63	68.25	69.50
2	59.33	49.45	69.48	56.68	69.50
3	64.24	50.55	78.30	62.68	69.50
4	57.84	49.45	78.31	61.43	69.50
5	49.85	50.67	78.28	57.56	69.50
6	51.71	53.71	78.29	61.19	69.50
7	58.01	50.55	68.44	61.83	69.50

TABLE IV. CLASSIFICATION RESULTS AT LOCATION B

Feature group	*Classification accuracy at LB (%)*				
	KNN	*NN*	*SVM*	*TREE*	*SSC*
1	68.55	89.74	89.05	89.52	86.47
2	70.81	59.01	88.62	62.76	86.47
3	65.22	40.99	84.52	64.83	86.47
4	73.36	59.01	84.50	72.57	86.47
5	70.86	59.24	84.53	60.35	86.47
6	68.55	89.74	89.05	89.52	86.47
7	70.81	59.01	88.62	62.76	86.47

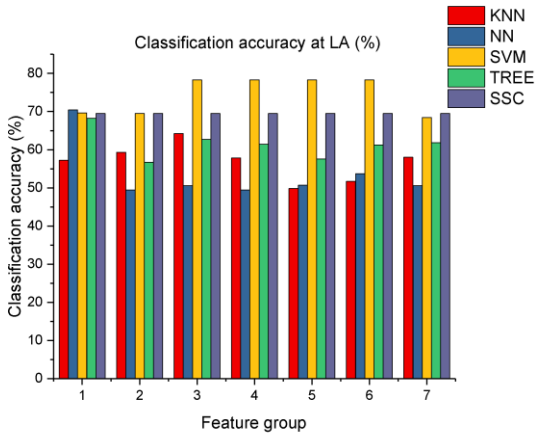

Fig. 10. Histogram results of classification accuracy for various methods at Location A.

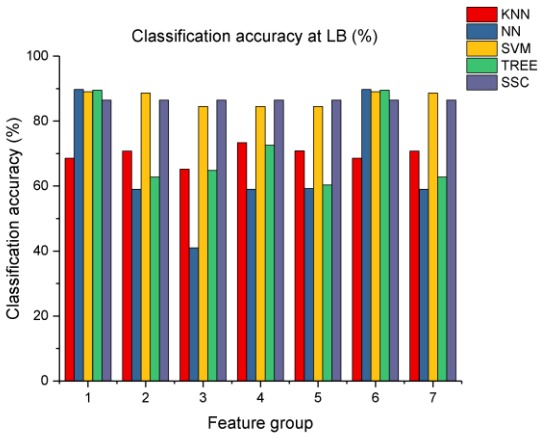

Fig. 11. Histogram results of classification accuracy for various methods at Location B.

TABLE V. POSITIONING RESULTS AT LOCATION A

Classification approach		*True label*	*ML*	*SSC*
Classification accuracy (%)		100	79.21	67.25
WLS (m)	*Mean error*	17.63		
	Standard error	9.59		
	Mean error in across-street direction	15.72		
	Mean error in along-street direction	6.91		
SM (m)	*Mean error*	9.12	10.09	16.71
	Standard error	5.96	4.56	4.43
	Mean error in across-street direction	2.16	6.06	7.33
	Mean error in along-street direction	8.58	7.19	14.47

TABLE VI. POSITIONING RESULTS AT LOCATION B

Classification approach		*True label*	*ML*	*SSC*
Classification accuracy (%)		100	85.90	85.18
WLS (m)	*Mean error*	19.22		
	Standard error	13.76		
	Mean error in across-street direction	17.92		
	Mean error in along-street direction	5.43		
SM (m)	*Mean error*	11.45	11.68	10.85
	Standard error	2.59	4.53	4.75
	Mean error in across-street direction	3.67	2.89	3.90
	Mean error in along-street direction	10.57	11.09	9.57

In terms of classification accuracy, two conclusions can be drawn.

First, the classification accuracy of SVM is about 12% higher than that of SSC, which is consistent with the machine learning results.

Second, it can be found that the classification accuracy of 79.21% for SVM with feature group 3 is higher than the maximum accuracy (78.31%) in Table III. This is because in the model and feature selection process, the pseudorange residual cannot be obtained with less than four satellites for one constellation according to (1), thus measurements of these satellites are ignored for all groups to maintain consistency. However, for shadow matching method, the pseudorange residual is not used, thus the sample number is bigger than that used in the selection process, which results in the different classification accuracy.

In terms of positioning results, due to its high classification accuracy, the poisoning results of SVM is very close to that of True label and better than that obtained using WLS. It is easy to find that a higher poisoning accuracy is obtained at the across-street direction than that at the along-street direction for shadow matching method, which is due to the inherent characteristic of shadow matching algorithm. Compared with shadow matching, the weighted least square method has a higher accuracy in along-street direction, but a lower accuracy in across-street. Thus, the integration of these two method can be further explored.

For results at Location B, only SNR is used as the feature for SVM because the best classification performance can be obtained using only SNR in this scenario according to Table VI. It can be found that the classification accuracy for ML and SSC is very high. But a slight performance decrease in positioning accuracy can be found for ML and True label, compared to SSC. A potential explanation to this phenomenon is that at some epochs, the classification results for the two methods are different, which are not necessarily reflected on classification accuracy. The different classification results would cause the

different positioning accuracy. Thus, it can be drawn that the classification accuracy is an imperfect metrics for evaluating machine learning performance. Another explanation is the effect of local Minima, which is shown in Fig. 6.

V. Conclusions and Future Work

The machine learning based on SVM has a unique advantage over other models according to the experiment results. Conclusions can be drawn as follows:

1) On the whole, machine learning performance is greatly affected by signal noise ration and elevation angle. Pseudorange residual improves the performance for most models (e.g. KNN, NN, TREE) in middle or mild urban environments. Pseudorange residual percentage and normalized pseudorange residual are two uncertain factors. They can increase or decrease the classification accuracy depending on the model and scenarios.

2) Features should be selected depending on the application scenarios. Signal noise to ratio can provide an acceptable performance in almost all cases. Besides, the accuracy of machine learning based on signal to noise ratio is higher than SSC. It should be noted that the classification accuracy would decrease due to the usage of elevation angle in deep urban areas. In middle or mild urban areas, however, it can improve the classification accuracy significantly.

3) Currently, the initial position for ML is provided by WLS, which is potentially affected by NLOS signals. The performance of ML would be further improved with a more accurate initial position, which can be calculated before excluding NLOS signals by ML.

4) The high accuracy of shadow matching method in the cross-street direction is further confirmed in this paper. Considering that the conventional weighted least square method has a better accuracy in along-street direction, a combination of the two methods has a potential better accuracy in both directions.

There are various kinds of SVM, which need analysis in future work. Besides, As shown in Table VI, the shadow matching method is easily affected by local Minima problem, which needs further exploration.

Acknowledgment

The authors acknowledge the fund of "Fundamental Research on Free Exploration Category of Shenzhen Municipal Science and Technology Innovation Committee (Project No. JCYJ20170818103653507)" to support this research.

References

[1] J. Joe Bradbury, "Prediction of urban GNSS availability and signal degradation using virtual reality city models", Proceedings of the 20th International Technical Meeting of the Satellite Division of The Institute of Navigation, Fort Worth, TX , pp 2696-2706, 2007.

[2] T.Pany, P. Pesec, and G.Stangl, "Atmospheric GPS slant path delays and ray tracing through numerical weather models, a comparison Pan", Physics and Chemistry of the Earth, Part A: Solid Earth and Geodesy, vol.26, pp.183-188, 2001.

[3] N. Viandier, D. F. Nahimana, J. Marais, and E. Duflos, "GNSS performance enhancement in urban environment based on pseudo-range error model", 2008 IEEE/ION Position, Location and Navigation Symposium, Monterey, CA, USA, pp.377-382, 2008.

[4] P. Groves, "Shadow Matching: A new GNSS positioning technique for urban canyons," Journal of Navigation, vol.64, pp.417-430, 2011.

[5] L.T. Hsu, H. Tokura, N. Kubo, Y. Gu, and S. Kamijo, "Multiple faulty gnss measurement exclusion based on consistency check in urban canyons", IEEE Sensors Journal, vol.17, pp.1909-1917, 2017.

[6] L. Wang, P.D. Groves, and M. K. Zieba, "Smartphone shadow matching for better cross-street GNSS positioning in urban environments", Journal of Navigation, vol.68, pp.411-433, 2015.

[7] M. Adjrad, and P.D. Groves, "Intelligent Urban positioning: integration of shadow matching with 3D-mapping-aided GNSS ranging" The Journal of Navigation, vol.71, pp.1-20, 2018.

[8] C. Ordóñez, J.R. Rodríguez-Pérez, J.J. Moreira, J.M. Matías, and E. Sanz-Ablanedo, "Machine learning techniques applied to the assessment of GPS accuracy under the forest canopy", Journal of Surveying Engineering, vol.137, pp.140-149, 2011.

[9] R.E. Guinness, "Beyond where to how: a machine learning approach for sensing mobility contexts using smartphone sensors", Sensors, vol.15, pp.9962-9985, 2015.

[10] Y. Jiao, J.J. Hall, and Y.T. Morton, "Automatic equatorial GPS amplitude scintillation detection using a machine learning algorithm" IEEE Transactions on Aerospace and Electronic Systems, vol.53, pp.405-418, 2017.

[11] L.T. Hsu, " Analysis and modeling GPS NLOS effect in highly urbanized area" GPS Solutions, vol.22, pp.1-12, 2018.

[12] L. Wang, P.D. Groves, and M.K. Ziebart, "GNSS shadow matching: improving urban positioning accuracy using a 3D city model with optimized visibility scoring scheme", NAVIGATION, Journal of The Institute of Navigation, vol.60, pp.195-207, 2013.

Authors

Haosheng XU

Mr XU received the bachelor degree in Thermal Energy and Power Engineering from Jilin University (JLU) , China, in 2016. He is currently a M.Sc. student at the Department of Mechanical Engineering, The Hong Kong Polytechnic University, Hong Kong. His research interests include deep learning-based GNSS localization, navigation and machine learning.

Guohao ZHANG

Dr. Guohao Zhang received the bachelor's degree in mechanical engineering and Automation from University of Science and Technology Beijing, China, in 2015. He received the master's degree in mechanical engineering and currently pursuing the Ph.D. degree in the Hong Kong Polytechnic University. His research interests including GNSS urban localization, vehicle-to-vehicle cooperative localization and multi-sensor integrated navigation.

Bing XU

Dr. XU received his B.S. and PhD. degrees in Network Engineering and Navigation Guidance and Control from Nanjing University of Science and Technology, China, in 2012 and 2018, respectively. He is currently a Postdoctoral Fellow with Interdisciplinary Division of Aeronautical and Aviation Engineering, The Hong Kong Polytechnic University. His research areas include signal processing in software-defined GNSS receivers and algorithm designing for GNSS/INS systems..

Li-Ta HSU

Dr. HSU received the B.S. and PhD. degrees in Aeronautics and Astronautics from National Cheng Kung University (NCKU), Taiwan, in 2007 and 2013, respectively. He was a Visiting Researcher with the Faculty of Engineering, University College London (UCL) and Tokyo University of Marine Science and Technology (TUMSAT), in 2012 and 2013, respectively. He was selected as a Japan Society for the Promotion of Sciences Postdoctoral Fellow with the Institute of Industrial Science, The University of Tokyo (UTokyo) and worked from 2014 to 2016. Dr. HSU currently are members of ION and IEEE and serve as a member of editorial board and reviewer in professional journal related to GNSS. He is currently an assistant professor with Interdisciplinary Division of Aeronautical and Aviation Engineering, The Hong Kong Polytechnic University.